MENOUFIYA UNIVERSITY
FACULTY OF ENGINEERING
ENG. RESEARCH BULL.
Vol. 17 Part I, 1994

PP. : 13: 29
Received at : 1 / 1 / 1994
Accepted at : 22 / 1 / 1994

AN INVESTIGATION INTO EIGEN-NATURE OF CONSTRAINED CRACKED BEAMS

BY

A.M. ABD EL-RAOUF* S.M. GHONEAM** AND M.H. BELAL***

* Prof. & Head of Department
** Associate. Prof. And *** Demonstrator
Production Engg.& Mech. Design Dept.,
Faculty of Engineering, Menoufia University, EGYPT.

ABSTRACT

It is known that the presence of cracks in structures introduces local flexibility associated with changes in the dynamic characteristics of structures. However the nature and variations of the natural frequencies due to the presence of cracks, are still under discussion and analysis.

The present work introduces an attempt to study the variations in the natural frequencies of uniform constrained beams due to different crack depths and locations. A theoretical and experimental investigation has been made. In the theoretical analysis, the nature of the cracks and their locations are modelled by introducing equivalent rotational and translational local flexibilities located through out the span of the beam. The numerical calculations of the eigen-frequencies are related to various stiffness ratios of these springs. From the otherhand, the experimental investigation is carried out-using Impact Hammer excitation and the Dual Channel Analyzer- to study the changes in the frequency response spectrums of constrained beams due to variations in the depth and the locations of cracks. The results are presented by using a proper fitting process. The coordination between the experimental and numerical results are carried out to investigate the equivalent stiffness corresponding to the depth of crack . Moreover, from the experimental results the damping characteristics of the cracked beam are computed by applying a half-power (bandwidth) method.

1. INTRODUCTION :

The vibration analysis of cracked beams and shafts is one of the most serious problems such as the case of turbomachinery. The appearance of cracks in machine elements and structures changes their physical and dynamical characteristics. The initiation of cracks can arise not only as a result of the accidental mechanical damage and the fatigue strength of materials but also due to improper environmental conditions and maintenance such as the occurance of erosion and corrosion. The lateral vibratory frequencies of single span beams having various combinations of classical geometrical and natural conditions moreover non-classical constraints have been evaluated.

Rutenberg [1] presented the results of the first three eigen-frequencies of a uniform cantilever beam with a rotational constraint at some point. Lau [2] introduced further study on a cantilever beam with an intermediate set of rotational and translational springs at some point. Maurize and De Rossit [3] obtained the fundamental frequency parameters of transverse vibrations of clamped-clamped beams with an intermediate translational constraint at various locations. Many researches utilized finite element techniques for the modelling of cracked structures and machines. In reference [4] Yuen used a reduced modulus of elasticity for the damaged element for changing the stiffness of the damaged cantilever beam. Rajab and Sabeeh [5] presented analytical expressions and derived curves relating the crack depth and location with the changes of the first natural frequencies. Qian et al. [6] used the integration of the stress intensity factors for deriving the element stiffness matrix of a beam with a crack. With the similar approach Sekhar and Prabhu [7] derived a local flexibility matrix on the basis of additional strain energy due to crack. Another approach was derived by Dimarogonas and Chondros [8] which modeled a crack at the built-in edge as a rotational spring. They investigated the relations between the change in the natural frequencies and both the local flexibilities and depth of crack for both a uniform cantilever beam and clamped-clamped beam. This approach has low computational effort and efficient results for the cases of cracked beams.

In the present work , An analytical and experimental investigations have been made for a constrained beam with various depths and locations of crack. In the present analytical analysis, the eigen-frequencies of an elastic constrained elements with various depths and locations of crack are expressed in terms of an equivalent set of rotational and translational spring elements. The computational results of the clamped-clamped beam with rotational and translational springs at various points are listed in proper graphical forms. In the experimental work, the crack is introduced successively at various depths and locations along the span of the beam. The

corresponding eigen-frequencies and amplitudes of vibration are measured using the Dual Channel Analyzer by utilizing an Impact Hammer excitation. The experimental results are listed in frequency domain form and the investigated graphs are presented by using the proper least square fitting process. From these graphs the damping characteristics due to crack propagation and location are determined using the half-power (bandwidth) method. Moreover, the coordination of analytical and experimental results permits the construction of the mathematical models of the translational and rotational stiffness of elastic elements. The values of the elastic elements parameters are determined for various cases of depth and location of the crack.

2. PROBLEM FORMULATION :

The partial differential equation of motion for free flexural vibration of elastic beam is governed by:

$$E\,I\,\frac{\delta^4 Y}{\delta x^4} + \rho\,A\,\frac{\delta^2 Y}{\delta t^2} = 0$$

Where E is flexural rigidity , I is moment of inertia ,
ρ is material density and A is cross-section area.

For small- amplitude of the vibratory constrained beam the ordinary differential equation characterized the deformed vibratory modes of the beam can be derived by the substitution the trial solution :

$$Y(x,t) = Y(x)\,.\,\cos(\omega\,t)\ ,$$

in the previous equation and the result is that:

$$E\,I\,\frac{d^4 Y}{dx^4} - m\,\omega^2\,Y(x) = 0$$

Where $m = \rho.A$ is mass per unit length.

Let consider an uniform beam be divided in two subdomains, characterized by the spatial coordinates u and v ,as shown in Fig. 1.

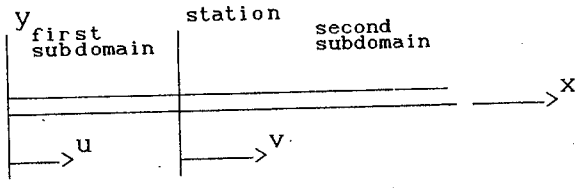

Fig.1- Beam of two subdomains u and v.

The characteristic equation for each subdomain, where $0 \le z \le 1$, can be written respectively as:

$$E\,I\,\frac{d^4 Y_1}{d\,u^4} - m\,\omega^2\,Y_1(u) = 0 \quad , \quad 0 < u < zL \qquad (1)$$

and

$$E\,I\,\frac{d^4 Y_2}{d\,v^4} - m\,\omega^2\,Y_2(v) = 0 \quad , \quad 0 < v < (1-z)L \qquad (2)$$

The general solutions of the ordinary differential Eqs. (1) and (2) for the first and second subdomains may be given respectively as :

$$Y_1(u) = c_1 \cosh \lambda u + c_2 \sinh \lambda u + c_3 \cos \lambda u + c_4 \sin \lambda u \qquad (3)$$

and

$$Y_2(v) = c_5 \cosh \lambda v + c_6 \sinh \lambda v + c_7 \cos \lambda v + c_8 \sin \lambda v \qquad (4)$$

Here the constants (c_i , i = 1,2,...,8) can be related to the type of the boundary conditions by imposing either the geometric and, or, natural boundary conditions for each subdomain.

3 . CASE STUDY : A Clamped-Clamped beam constrained by a set of rotational and translational springs :

Consider a translatory rotational constrained clamped-clamped beam of total length L, flexural rigidity E, moment of inertia I and the material density is ρ, as shown in Fig. 2. Here K_T and K_R are the translational and rotational spring stiffnesses, respectively.

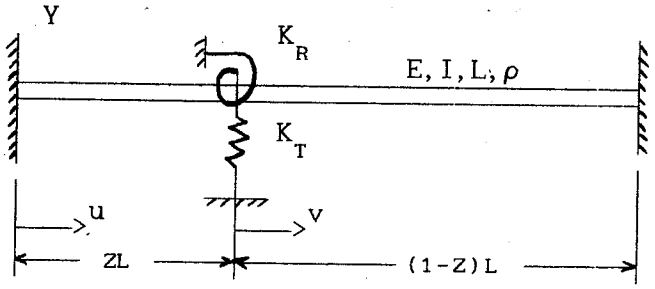

Fig. 2- Translatory rotational clamped-clamped beam.

3-1 . Boundary Conditions:

Here the boundary conditions for the first subdomain are defined as:

At u = 0 :
$$Y_1 = 0 \quad , \quad \frac{d\,Y}{d\,u} \qquad (5)$$

At u = zL :

$$E\,I\,\frac{d^2Y_1}{d\,u^2} = +\,S_r\,K_R\,\frac{d\,Y_1}{d\,u} \qquad 0 \le S_r \le 1 \qquad (6\text{-a})$$

$$E\,I\,\frac{d^3Y_1}{d\,u^3} = -\,S_t\,K_T\,Y_1 \qquad 0 \le S_t \le 1 \qquad (6\text{-b})$$

Where $S_r K_R$ and $S_t K_T$ are the components of the rotational and translational spring stiffnesses, respectively, attached for the first subdomain.

The boundary conditions for the second subdomain are:

At $v = 0$:

$$E\,I\,\frac{d^2Y_2}{dv^2} = -(1-S_r)\,K_R\,\frac{dY_2}{dv} \qquad (7\text{-a})$$

$$E\,I\,\frac{d^3Y_2}{dv^3} = +(1-S_t)\,K_T\,Y_2 \qquad (7\text{-b})$$

At $v = (1-z)L$:

$$Y_2 = 0\ ,\quad \frac{dY_2}{dv} = 0 \qquad (8)$$

Thus the compatibility conditions at the station at which the beam is divided into the two subdomains are given by:

$$Y_1 = Y_2\ ,\quad \frac{dY_1}{du} = \frac{dY_2}{dv} \qquad (9)$$

Taking into account both the boundary conditions (6) and (7) and the compatibility condition (9). The imposing conditions for the translatory rotational station can be summarized as :

$$E\,I\,\frac{d^2Y_1}{du^2} = +K_R\,\frac{dY_1}{du} + E\,I\,\frac{d^2Y_2}{dv^2} \qquad (10)$$

and

$$E\,I\,\frac{d^3Y_1}{du^3} = -K_T Y_1 + E\,I\,\frac{d^3Y_2}{dv^3} \qquad (11)$$

The imposing conditions for the whole beam contained the equations (5), (8), (9), (10), and (11).

3-2 . Characteristic Equation :

Substituting equations (3) and (4) in the imposing condition (5), (8), (9), (10), and (11) results a linear system of homogeneous equations expressed in terms of the unknown constants c_i ,

$$[D_{ij}(\lambda)]\,[c_i] = 0\ ,\quad i,j = 1,2,\ldots 8 \qquad (12)$$

For a non-trivial solution, the determinant of the coefficient matrix must be vanished and the frequency equation can be obtained in the form :

$$\left| D_{ij}(\lambda) \right| = 0 \qquad (13)$$

where:

$D_{11} = D_{13} = 1$, $D_{12} = D_{14} = D_{15} = D_{16} = D_{17} = D_{18} = 0$

$D_{22} = D_{24} = 1$, $D_{21} = D_{23} = D_{25} = D_{26} = D_{27} = D_{28} = 0$

$D_{31} = \cosh(zB)$, $D_{32} = \sinh(zB)$, $D_{33} = \cos(zB)$

$D_{34} = \sin(zB)$, $D_{35} = D_{37} = -1$, $D_{36} = D_{38} = 0$

$D_{41} = \sinh(zB)$, $D_{42} = \cosh(zB)$, $D_{43} = -\sin(zB)$

$D_{44} = \cos(zB)$, $D_{46} = D_{48} = -1$, $D_{45} = D_{47} = 0$

$$D_{51}= \cosh(zB)-\frac{R}{B}\sinh(zB) \quad , \quad D_{52}= \sinh(zB)-\frac{R}{B}\sinh(zB)$$

$$D_{53}= -\cos(zB)+\frac{R}{B}\sin(zB) \quad , \quad D_{54}= -\sin(zB)-\frac{R}{B}\cos(zB)$$

$$D_{55}= -1 \quad , \quad D_{57}= 1 \quad , \quad D_{56}= D_{58}= 0$$

$$D_{61}= \sinh(zB)+\frac{T}{B^3}\cosh(zB) \quad , \quad D_{62}= \cosh(zB)+\frac{T}{B^3}\sinh(zB)$$

$$D_{66}= -1 \quad , \quad D_{68}= 1 \quad , \quad D_{65}= D_{67}= 0$$

$$D_{63}= \sin(zB)+\frac{T}{B^3}\cos(zB) \quad , \quad D_{64}= -\cos(zB)+\frac{T}{B^3}\sin(zB)$$

$$D_{71}= D_{72}= D_{73}= D_{4}= 0 \quad , \quad D_{75}= \cosh(1-z)B$$

$$D_{76}= \sinh(1-z)B \quad , \quad D_{77}= \cos(1-z)B \quad , \quad D_{78}= \sin(1-z)B$$

$$D_{81}= D_{82}= D_{83}= D_{84}= 0 \quad , \quad D_{85}= \sinh(1-z)B$$

$$D_{86}= \cosh(1-z)B \quad , \quad D_{87}= -\sin(1-z)B \quad , \quad D_{88}= \cos(1-z)B$$

$$B = \lambda L \quad , \quad R = K_R L/EI \quad \text{and} \quad T = K_T L^3/EI$$

For the limiting case at which R and T tends to infinity, the characteristic equation (13) reduced to the classical frequency equation for the case of the clamped-clamped beam [9].when z = 0 and T tends to infinity , equation (13) reduces to the frequency equation for the clamped-clamped beam with crack at one clamped edge as stated in ref.[8].

At any location of the translatory rotational constraint, substituting the eigen- frequency parameters obtained from Eq.(13) into the eigenvalue problem (12) to determine the constants c_{ir} (r=1,2,..,5) related to the corresponding mode.

Consequently, the r_th mode shape can be then obtained in terms of the obtained coefficients c_{ir} from equations (3)and (4) here as:

$$Y_{1r}(u)= c_{1r}\cosh \lambda_r u + c_{2r}\sinh \lambda_r u + c_{3r}\cos \lambda_r u + c_{4r}\sin \lambda_r u$$

and

$$Y_{2r}(v)= c_{5r}\cosh \lambda_r v + c_{6r}\sinh \lambda_r v + c_{7r}\cos \lambda_r v + c_{8r}\sin \lambda_r v$$

4 . EXPERIMENTAL WORK :

4-1 . Specification and instrumentation set :

In the present experimental analysis seven specimens with different crack locations are considered. The seven specimens steel beams are made of the same material with the same dimensions L= 800 mm.(where L is the length of the beam) and

W*H= 12*12 mm. (where W and H are the width and depth of cross section respectively). The ends of the specimen are fixed by two thick steel plates of very high stiffness using the same procedure of the manual shielded metal-arc welded technique. The two thick steel plates are clamped with the vertical stands by using bolts and nuts to ensure proper fixation. The crack was initiated for each beam with a saw cut and propagated successively with 1.5 mm. step . At each step the depth of the crack is checked directly by the measurement. The crack locations for the seven samples are chosen at left end, and 0.1, 0.2 ,0.25 ,0.3 ,0.4 and 0.5 of the span from the left end of each beam respectively. For the symmetrical boundary conditions at both sides of the beam, the same affect of length ratio (e.g. Lc/L=0.3 and 0.7) with respect to the first mode occurs at the same ratio of depth of crack, where Lc is the length of the beam segment to the left of the crack site.

The measurement set includes a fabricated test rig and instrumentation set-up formed from excitation and measuring systems of Bruel and Kjaer products as shown in Fig. (3-a). A photograph of actual experimental layout is shown in Fig. (3-b). In the figure, the Impact Hammer (type 8202) which resembles an ordinary hammer but has a force transducer (type 8200) built into the tip to register the force input is used to excite the sample at mid-point position. A tap with the hammer imparts a pulse with a broad frequency range to the test sample. This will simultaneously excite all the modes of vibration. The signal from the force transducer in the hammer head is routed via a Preamplifier to the measurement instrumentation. The line drive preamplifier (type 2644) can be mounted directly onto the handle of the Impact Hammer. The Charge Amplifier (type 2635) is used to generate the signal from the hammer to the Dual Channel Analyzer (type 2034) at channel A. For measuring the response parameters, a Piezoelectric Accelerometer (type 4367) is mounted by a smaller magnet on the sample. The Accelerometer is characterized by measuring the displacement level from 0.002 to 10.0 mm. with natural frequency range upto 29 KHz. The Vibration Meter (type 2511) is utilized in connection with the Accelerometer to generate the signal to the Dual Channel Analyzer at B. The frequency response spectrum can be obtained from the printer which is supported by the Desktop Computer series the Dual Channel Analyzer.

4-2. The experimental procedure :

After the calibration of instrumentation set and the ensurance of the proper isolation of the test rig from undesired sources of excitation are established, the procedure of measurements includes mainly: -

-The locations of the Impact Hammer excitation and Accelerometer mounting points are chosen in the mid-point of the span of the constrained beam.

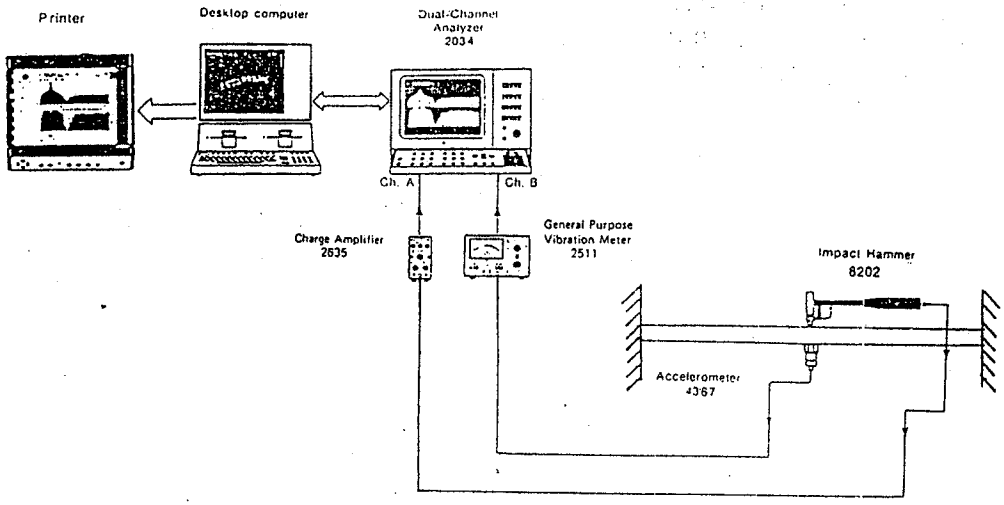

(a) Schematic diagram of the test set-up.

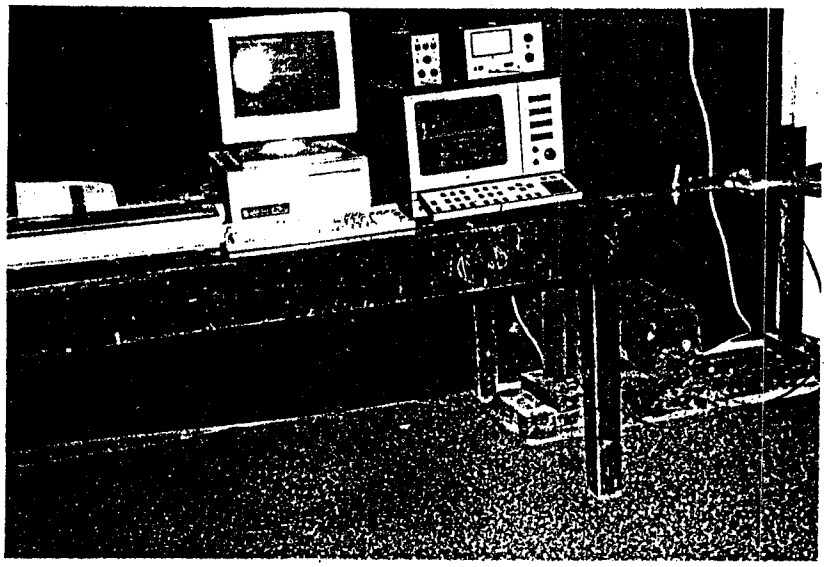

(b) Overall view of the actual test set-up.

Fig.3- Instrumentation set-up for monitoring the frequency response spectrum.

-The measurements of a frequency response spectrum of the beam without crack within the range 0 to 800 Hz. is plotted as a reference of the zone of the natural frequencies and the associated amplitudes of vibrations.
-At the current crack location, the depth of crack propagates increased and the frequency response spectrums at each depth of crack are plotted.
-The same procedure of measurement is repeated for each crack locations.

5 . RESULTS AND DISCUSSION:

The computational results can be carried out with several combinations of rotational and translational spring ratios at various locations of the presented model. The natural frequencies of the cracked beam under consideration are determined numerically by solving the characteristic equation of the beam; Eq. (13). Figure (4) displays the variation of the fundamental eigen-frequencies for different local flexibility locations and rotational spring ratios within the range $1 \leq R \leq 200$ and for different translational spring ratioes. For large rotational spring ratio ($R \geq 120$), it is noticed that as R increased the frequency ratios are approximately invariant. In a similar manner, Fig. (5) displays the variation of the fundamental eigen-frequencies with translational spring ratios within the range $1 \leq T \leq 200$ and different rotational spring ratios for different locations. From the graphs (4) and (5), it is clear that the rate of the change of T is relatively large compared with the rate of change of R. In addition, it is evident that in the bending vibration mode, the translational spring element (in corresponding to shear criteria) is play important role in the first mode rather than the rotational spring element (in corresponding to flexural criteria). In general, it is clear that the frequency ratio depends on the stiffness ratios R and T.

In the experimental results, the frequency response spectrum for the typical values of Hc/H ratio and for various positions of crack Lc were determined samples of these results for mid-point position of creak being shown in Fig. (6) from the figure, it is noticed that for the current depth ratio and length ratio, the smaller changes of the natural frequencies will be the order of the higher frequencies. The flexability of the creaked beam depends also on the amplitude ratio at which the creak occurs. Based on the assumption of a transverse, surface creak, extending uniformly along the width of the beam. Figures (7) and (8) represent graphically the quantitative relationships of depth and location of the crack versus the change of fundamental natural frequency. In addition, the variation of maximum amplitudes of the first mode shape versus the depth of the crack were determined in Fig. (9). In the present study, the damping coefficients are evaluated directly by experimental methods. The half-power (bandwidth) method is sufficient and suitable for the

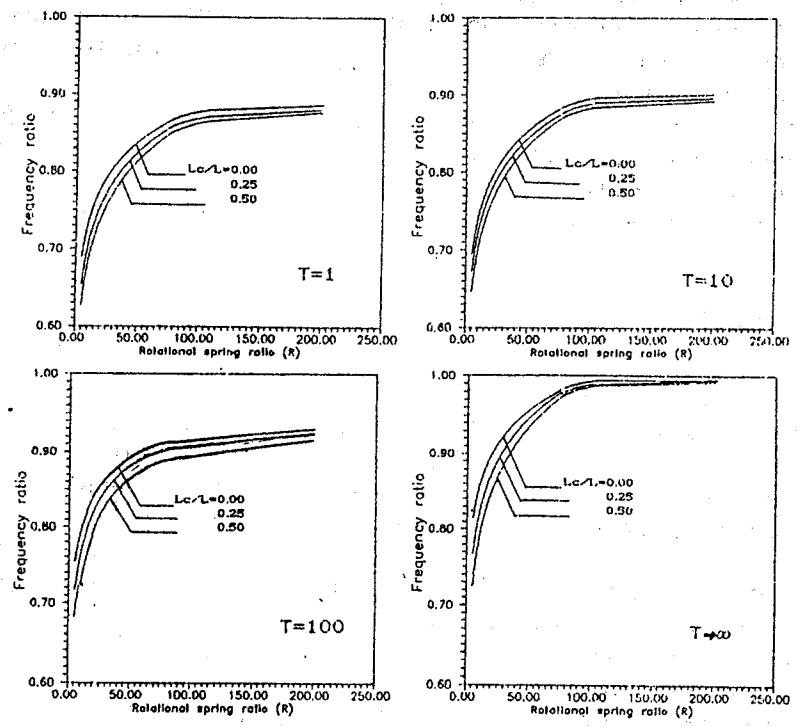

Fig.4- Variation of the fundamental frequency with R for various values of T and different locations.

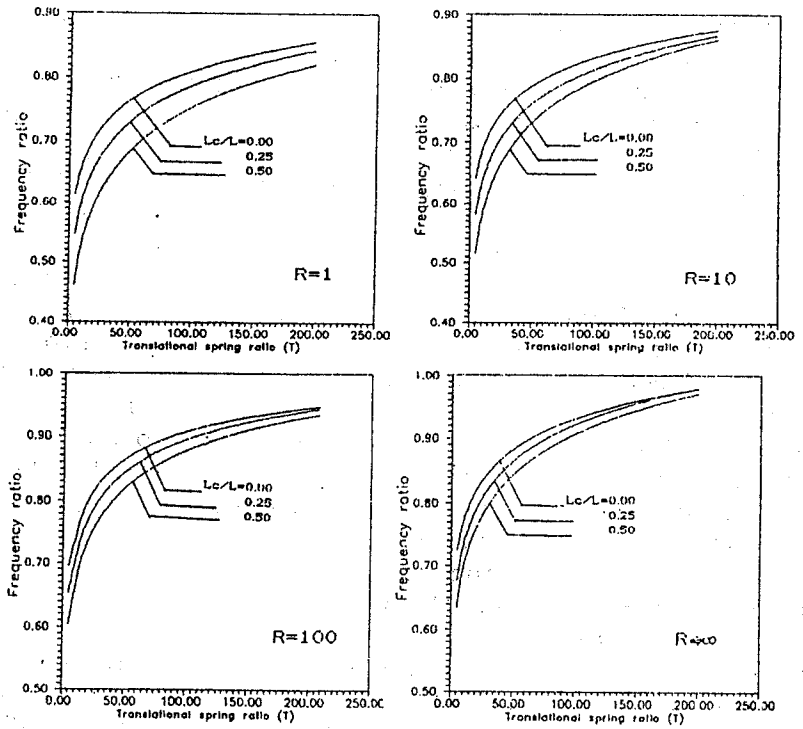

Fig.5- Variation of the fundamental frequency with T for various values of R and different locations.

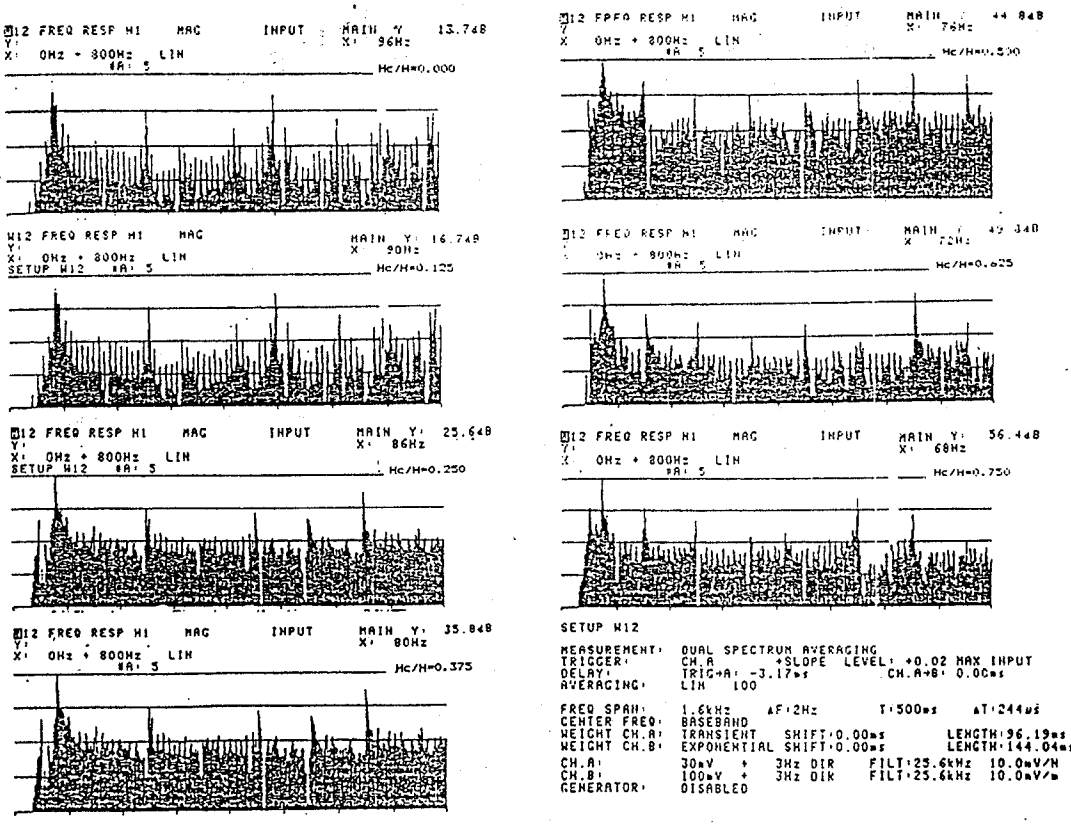

Fig.6- Frequency response spectrums for the various values of Hc/H ratio at the mid-point location of the span.

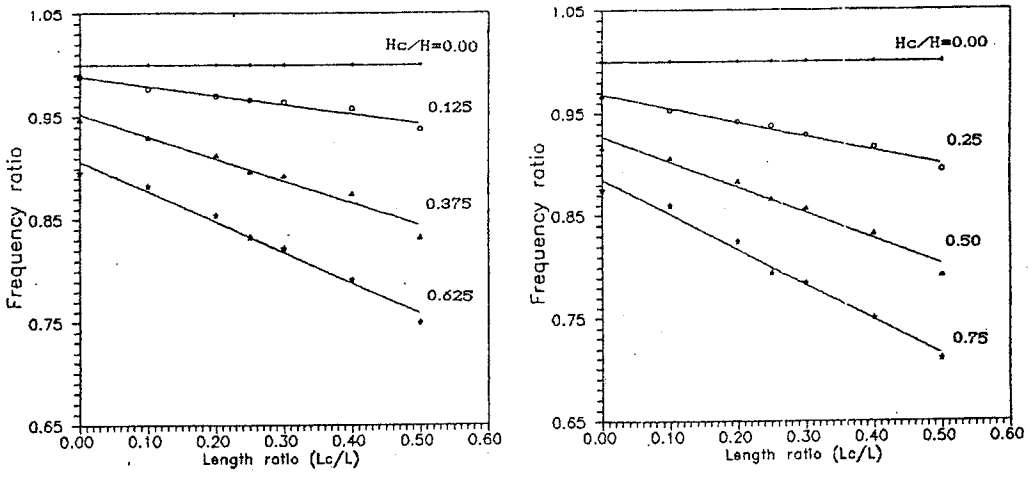

Fig.7- Variation of the fundamental frequency of cracked beam versus the depth of crack ratio and the location of crack ratio.

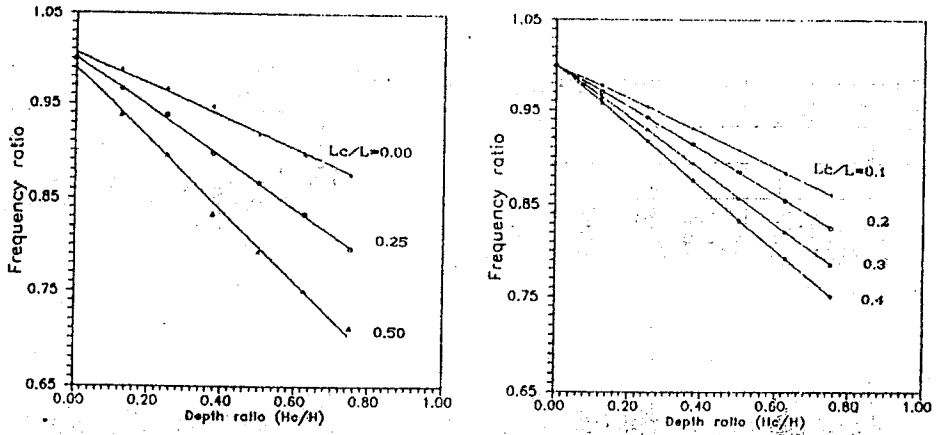

Fig.8- Variation of the fundamental frequency of cracked beam versus the location of crack ratio and the depth of crack ratio.

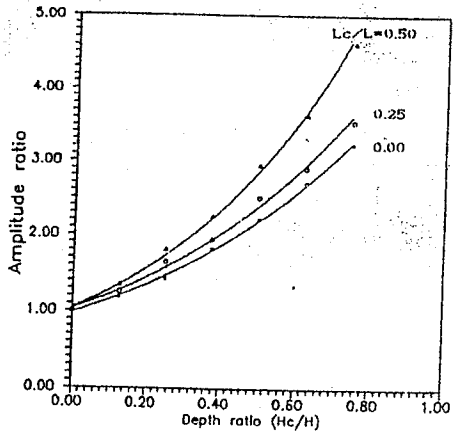

Fig.9- Variation of amplitude ratio at various location of crack ratio with various depth of crack ratio.

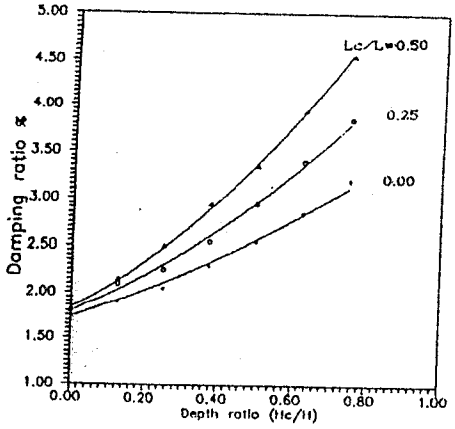

Fig.10- Variation of damping ratio at various location of crack ratio with various depth of crack ratio.

light damping ratio less than 0.05 as shown in Ref.[10]. The damping ratio of clamped-clamped beam with various depth and location of the crack were measured and the results being shown in Fig.(10).

The proper fitting curves for the experimental results are obtained by the use of least square fitting process and the results :

1- Linear form as: $Y = A_1 + A_2.X$

where Y and X represent frequency ratios and (Lc/L) or (Hc/H) respectively and :

2- Exponential form as: $Y = A_1.Exp(A_2.X)$

where Y and X represent damping ratios % or amplitude ratios and (Hc/H) respectively. The coefficients A_1 and A_2 are tabulated as shown in tables (1) and (2).

In figures (7) and (8) it is shown that the frequency of vibration is linearly decreases with increasing the depth of crack for the example in case of Lc/L=0.5 and Hc/H=0.75, the frequency of vibration is 0.71 times smaller than in the case of vibration without crack furthermore, the variations of measurement of maximum amplitudes of the first mode shape are increased exponentially with increasing the depth of crack, as shown in fig.(9). For the example in case of Lc/L=0.5 and Hc/H=0.75, the amplitude of vibration is 4.6 times bigger than in the case of vibration without cracks. It should be observed that for small cracks (e.g. for Lc/L=0.0 and Hc/H=0.125 and even for Lc/L=0.2, Hc/H=0.25) the changes of amplitude of vibration and of the frequency are relatively small compared with other locations and depths of cracks. The fundamental frequency decreases when the crack occurs close to the middle of considered beam where the maximum amplitude of the mode shape occurs. This is expected since maximum amplitude at the first mode occurs at the crack location. It is clear from Fig.(10) that the damping capacity of cracked beam increased exponential with increasing the depth of crack (e.g. for Lc/L=0.5 and Hc/H=0.75, the damping ratio is 2.5 times bigger than in the case of vibration without cracks), since the larger depth of crack, the larger amount will be the dissipation of energy.

Table (1): Coefficients for linear fitting results

Fig.(5)			Fig.(6)		
Hc/H	A_1	A_2	Lc/L	A_1	A_2
0.000	1.000	0.000	0.00	1.006	-0.176
0.125	0.988	-.089	0.10	1.001	-0.187
0.250	0.968	-.136	0.20	1.001	-0.223
0.375	0.952	-.215	0.25	0.999	-0.273
0.500	0.927	-.253	0.30	0.999	-0.287
0.625	0.907	-.295	0.40	0.998	-0.333
0.750	0.885	-.314	0.50	0.995	-0.385

Table (2): Coefficients for exponential fitting results

Fig. (7)			Fig. (8)		
Lc/L	A1	A2	Lc/L	A1	A2
0.00	0.979	1.606	0.00	1.735	0.787
0.25	1.031	1.684	0.25	1.794	1.006
0.50	1.044	2.019	0.50	1.831	1.226

Under the similar boundary conditions, the experimental and numerical results, one can made an coordination between these results to investigate eigen-nature of the cracked beam. For the cracked present model, table (3) was constructed relating directly the depth of crack to the equivalent stiffness ratios at different locations. From the experimental results shown in Fig. (8), it can found that the effect of the depth and location of crack on the frequency ratio have linear nature with monotonic decreasing trend. On the obtained, from the graphs in figures (4) and (5) at the same frequency ratio, on can be determined successfully the equivalent stiffness ratios and damping ratio; see table (3). The results is that the increasing

Table (3) : The coordination between the depth of crack and dynamic characteristics for different locations (within $1 \leq R$ & $T \leq 200$).

Length ratio (Lc/L)	Depth ratio (Hc/H)	Equivalent stiffness ratios								Damping ratio %
		R=1	T=1	R=10	T=10	R=100	T=100	R⇒∞	T⇒∞	
		T	R	T	R	T	R	T	R	
0.00	0.125								82	1.90
	0.250							169	58	2.05
	0.375						195	129	43	2.30
	0.500						77	83	27	2.55
	0.625				190	156	53	61	19	2.85
	0.750		89	200	69	109	38	45	14	3.20
0.25	0.125							177	65	2.01
	0.250							125	45	2.25
	0.375					128	65	76	26	2.56
	0.500		87	200	68	116	42	52	18	2.95
	0.625	180	56	132	44	72	26	35	12	3.40
	0.750	115	34	82	27	42	15	22	7	3.85
0.50	0.125							142	52	2.12
	0.250					183	71	89	33	2.50
	0.375		63	147	49	85	33	45	17	2.95
	0.500	148	38	95	30	51	20	29	11	3.35
	0.625	96	23	60	18	31	12	18	7	3.95
	0.750	64	14	40	11	19	7	12	5	4.55

the depth of crack decreases both the rotational and translational spring ratios. From the practical point of view, the present method can be developed as a useful tool for preventive maintenance and non-destructive testing of structures. The quantitative dimensionless results given in the present study are strictly applicable to a particular case of simple geometry, but accordingly can be applied to individual members of large structures. For the general case of a complex structure, the structural analyst however can use this analysis as a guide to obtain quantitative results.

6. CONCLUSIONS :

Experimental set-up and mathematical model for investigated the effects of crack propagation and its location of clamped-clamped beam on the fundamental frequency, amplitude and damping has been studied. In addition, the present method provides an efficient non-destructive tool for testing each individual components of any mechanical system. The following, summarizes the conclusions drawn from the analytical and experimental studies and the coordinations between them :

1- The influence of crack on the eigen-frequencies and corresponding amplitudes with respect to the uncracked beam, depending on the location and magnitude.

2- The fundamental frequency ratio decreases linearly when the crack occurs close to the middle of clamped-clamped beam where the maximum amplitude of the mode shape occurs.

3- The damping capacity of cracked beam are increases exponentialy with increasing the depth of crack (due to the dissipation of energy).

4- In the bending first mode the translational spring elements have dominant affect compared with the rotational spring elements.

5- The coordination between the experimental and analytical results to determine the equivalent rotational and translational stiffness due to crack propagation is becoming stronger due to the introducing of suitable hybrid analytical-experimental approaches.

REFERENCES

[1] A. Rutenberg, (1978) "Vibration frequencies for a uniform cantilever with a rotational constraint at a point." J. of Applied Mechanics, 45, pp 422-423.

[2] J.H. Lau, (1984), "Vibration frequencies and mode shapes for a constrained cantilever." J. of Applied Mechanics, 51, pp 182-187.

[3] M.J. Maurizi and D.V. Bambil De Rossit, (1987) "Free vibration of a clamped-clamped beam with an intermediate elastic support." J. of Sound and Vibration, 119(1), pp 173-176.

[4] M.M.F. Yuen, (1985) "A numerical study of the eigen-parameters of a damaged cantilever." J. of Sound and Vibration, 103(3), pp 301-310.
[5] M.D. Rajab and A. Al Sabeeh, (1991) "Vibration characteristics of cracked shafts." J. of sound and Vibration, 147, pp 465-473.
[6] G. L-Qian, S-N. Gu and J-S. Jiang, (1990) "The dynamic behaviour and crack detection of a beam with a crack." J. of Sound and Vibration, 138, pp 233-243.
[7] A.S. Sekhar and B.S. Prabhu, (1992), "Crack detection and vibration characteristics of cracked shafts." J. of Sound and vibration, 157(2), pp 375-381.
[8] A.D. Dimorogonas and T.G. Chondros, (1980) "Identification of cracks in welded joints of complex structures." J. of Sound and Vibration, 69(4), pp 531-538.
[9] R.E.D. Bishop and Johnson, (1979), "The Mechanics of Vibration." Cambridge University Press.
[10] K. Zaveri and M. Phil, (1985), "Modal Analysis of large Structures." Brul & Kjaer.

دراسة الأداء الديناميكى للأعتاب المقيدة ذات الشروخ

ا.د / أحمد ماهر عبد الرؤوف
د/ صبحى غنيم و م/ محمد هشام بلال

الملخص العربى

يعد ظهور الشروخ فى المنشآت وأجزاء وقواعد الماكينات من المشاكل الخطيرة لما يحدثه من تغيرات فى أدائها الديناميكى نتيجة لتغيير خواص الكزازة .

ولمعرفة تأثير موضع الشروخ وعمقها على الأداء الديناميكى للأعتاب المقيدة تمت دراسة نظرية وعمليه على أعتاب مقيدة ذات شروخ محتلفة الموضع والعمق . وتم تمثيل النموذج الرياضى للشروخ بمجموعة مكافئة من الياءات الإلتوائية والمستعرضة . وتم استخدام الحاسب لإيجاد النتائج الخاصة للترددات الطبيعية للأعتاب ذات الشروخ المتنوعة . ومن الناحية العملية تم قياس وتحليل النتائج الخاصة بالترددات ونسب الإخماد لمجموعة عينات متماثلة من الأعتاب المقيدة ذات شروخ مختلفة فى الموضع والعمق.

وقد تم استنتاج علاقات تجريبية باستخدام (fitting process) تربط بين قيمة التردد الطبيعى الأول للأعتاب المقيدة ذات الشروخ التى تقل مع زيادة عمق الشرخ والقرب من منتصف العتب المقيد عنها للأعتاب بدون شروخ بعلاقة خطية . كما تم استنتاج علاقات تربط بين زيادة قيمة الإهتزازة العظمى والحاجة إلى إخماد الإهتزازات مع زيادة عمق الشرخ والقرب من منتصف العتب المقيد بعلاقة أسية . وتمت المقارنة بين نتائج الحاسب والقياسات العملية لإيجاد قيم معامل الكزازة للياءات المكافئة لمواضع وعمق الشروخ .

وقد احتوى البحث على وسيلة غيرإتلافية لإختبار وصيانة المنشآت وأجزاء الماكينات ذات الشروخ باستخدام الربط بين نتائج الحاسب والقياسات العملية .